Plant Physiol. (1990) 94, 840–849
0032-0889/90/94/0840/10/$01.00/0

Received for publication March 7, 1990
Accepted June 16, 1990

A Water Relations Analysis of Seed Germination Rates[1]

Kent J. Bradford

Department of Vegetable Crops, University of California, Davis, California 95616

ABSTRACT

Seed germination culminates in the initiation of embryo growth and the resumption of water uptake after imbibition. Previous applications of cell growth models to describe seed germination have focused on the inhibition of radicle growth rates at reduced water potential (ψ). An alternative approach is presented, based upon the timing of radicle emergence, to characterize the relationship of seed germination rates to ψ. Using only three parameters, a 'hydrotime constant' and the mean and standard deviation in minimum or base ψ among seeds in the population, germination time courses can be predicted at any ψ, or normalized to a common time scale equal to that of seeds germinating in water. The rate of germination of lettuce (*Lactuca sativa* L. cv Empire) seeds, either intact or with the endosperm envelope cut, increased linearly with embryo turgor. The endosperm presented little physical resistance to radicle growth at the time of radicle emergence, but its presence markedly delayed germination. The length of the lag period after imbibition before radicle emergence is related to the time required for weakening of the endosperm, and not to the generation of additional turgor in the embryo. The rate of endosperm weakening is sensitive to ψ or turgor.

Seed germination is the process of initiating growth of a previously quiescent or dormant embryo. For most seeds, it begins with imbibition of water. Imbibition is generally a triphasic process, with rapid initial water uptake (phase I), followed by a plateau phase with little change in water content (phase II), and a subsequent increase in water content coincident with radicle growth (phase III) (3). In terms of the regulation of germination, phase II is of primary interest, since germination in the physiological sense can be considered to be completed when embryo growth is initiated. It is the length of phase II that is generally extended by dormancy, low or high temperatures, water deficit, or abscisic acid, while factors which promote germination do so by shortening this lag phase. Once the radicle has penetrated any enclosing tissues and is growing, germination is complete and seedling growth has begun.

A number of attempts have been made to apply the Lockhart (19) model for plant cell growth to the initiation of radicle growth during seed germination (*e.g.*, 5, 21, 23, 29). The Lockhart model describes cell growth by the empirical equation

$$dV/Vdt = m(\psi_p - Y), \quad (1)$$

where dV/Vdt (Table I) is the rate of volume increase relative to the total volume, m is an extensibility coefficient relating growth rate to ψ_p, ψ_p is the turgor pressure, and Y is the minimum or threshold turgor that must be exceeded for growth to occur. Since water uptake is required for the volume increase during growth, growth rate is also described by

$$dV/Vdt = L(\psi - \psi_i), \quad (2)$$

where L is the hydraulic conductance of the tissue (incorporating pathway geometry, usually unknown), ψ is the water potential of the external medium, and ψ_i is the water potential of the growing cell. These two equations can be combined to give

$$dV/Vdt = \frac{L \cdot m}{L + m}(\Delta\psi + \psi_p - Y), \quad (3)$$

where $\Delta\psi$ is $\psi - \psi_i$. When $L \gg m$, this equation reduces to Equation 1, as $\Delta\psi$ is small when L is large. If $m \gg L$, then the equation reduces to Equation 2, as L and $\Delta\psi$ will control the rate of growth by determining the rate of water transport (2, 4, 6). In the case of seed germination, where growth is initiated at the end of a period of near equilibrium between the seed ψ and its surroundings, $\Delta\psi$ will be small (3, 15, 23, 29, 30). As the distances for water transport are also small, and the water uptake rates during phase I of imbibition usually far exceed those required to sustain growth, it is unlikely that growth is limited by L. Thus, Equation 1 has been used to describe and interpret the water relations of seed germination (4, 5, 21, 22, 29).

The application of Equation 1 is simple only under near steady-state conditions (constant rate of growth) when m, Y, and cellular osmotic potential (ψ_π) are assumed to be constant (4). Carpita *et al.* (5) utilized growing excised embryonic axes of lettuce (*Lactuca sativa* L.) to estimate the parameters of Equation 1. A difference in external ψ of 0.34 MPa was required to maintain equal constant growth rates of red- and far-red-irradiated embryonic axes. The difference was attributed equally to a lower ψ_π (which would increase ψ_p) and to a larger m (more extensible cell walls) in red-irradiated seeds. However, the data fit the model of Equation 1 rather poorly, apparently indicating that some of the parameters of the equation were changing during the incubation of axes at a range of ψ values. Schopfer and Plachy (23) used a similar approach to study the water relations of rape (*Brassica napus* L.) seed germination. They imbibed seeds for varying periods on water, then determined the linear rates of water uptake or loss over 12 h after transfer to solutions of different ψ. From these data, they concluded that m increased markedly and Y fell to zero when radicle growth was initiated. However, these

[1] Supported by National Science Foundation grant DCB88-17758 and by grants from the California Iceberg Lettuce Research Board and the Western Regional Seed Physiology Research Group.

results are difficult to interpret because in some cases the changes in seed volume apparently represented irreversible growth, while in others reversible shrinking and swelling were being measured. Thus, it is likely that the cell wall properties being evaluated (*i.e.* the elastic versus plastic extensibility) differed depending upon the ψ of the external solution, as was evidenced by discontinuities in the growth rate versus ψ curves as growth rate neared zero (23). A more fundamental problem with applying these approaches to the initiation of embryo growth is that during phase II, growth is not occurring, so m and Y cannot be evaluated. Once growth is initiated, m and Y can be evaluated, but the seeds are then in phase III, and the parameters will refer to cell growth rather than to germination *per se*. The objective in applying growth models to seed germination is generally to investigate how various factors, such as ψ, temperature, light, or growth regulators, influence the initiation of radicle growth, not how they influence subsequent root growth rates.

An alternative approach is to use radicle emergence as the criterion that growth has been initiated and germination completed, and then quanitiate the ψ required to inhibit germination, or reduce growth rate to zero. At this ψ, $\psi_p = Y$, or $Y = \psi - \psi_\pi$, assuming ψ and ψ_i are essentially equal and $\psi_p = \psi_i - \psi_\pi$. The ψ_π at this ψ, rather than at full imbibition, must be determined, either directly, or by accounting for the changes in embryo volume as ψ is reduced (3). Thus, Y (or the ψ_p remaining when germination is just prevented), but not m, can be quantified by this approach (17, 23, 26, 29). However, caution must be exercised in applying this method, as it is possible that Y itself may change during the lengthy incubations necessary to determine the ψ that inhibits final germination (8), since reductions in ψ progressively delay germination, even though the final percentage of germination may be unaffected (8, 16, 23).

In many seeds, the embryo is surrounded by endosperm, perisperm, or other tissues that may restrict radicle growth (8, 12, 28–30). A satisfactory model of seed germination rates should be able to account for, and quantitate, the influence of such enveloping tissues. This has been done only by the germination inhibition approach, comparing intact seeds to embryos from which the enclosing tissues have been removed (15, 17, 21, 26, 29, 30). Some estimates of the contribution of enclosing tissues to Y (*i.e.* Y_e) have been obtained by this method, but the cautions cited above apply to these data as well. Y_e has also been estimated from the force required to puncture through the endosperm (8, 13, 21, 28), and while the values obtained correlate well with final germination responses, it is difficult to relate them quantitatively to ψ or to germination rates within the seed population.

A final limitation of previous applications of growth models to seed germination rates lies in their inability to account for the discontinuous nature of seed germination. The Lockhart model was originally developed to describe single cells, and has been adapted to the growth of tissues (2, 4, 6, 27). Growth in these systems is a continuous variable, whereas seed germination is a discrete variable, since at a given time, an individual seed has either germinated or it has not. However, the times to germination of seeds within a population can be described in statistical terms, as in the mean and variance of germination times (25), and these parameters can then be considered as continuous variables reflecting the response of the seed population to environmental influences. If the Lockhart model is to be applied to germination, it must be modified to account for the special characteristics of seed populations.

I describe here an alternative approach to the application of growth models to seed germination. Statistical methods appropriate to the study of population distributions of quantal responses are employed to derive quantitative parameters that characterize germination responses to ψ. These parameters can then be used to predict germination rates and final germination percentages at any ψ. By estimating the embryo ψ_p at different ψs, a model relating seed germination rates to ψ_p can be developed that is formally analogous to the cellular growth models, but is based on the rates of initiation of radicle growth within the seed population rather than on water uptake rates.

Table I. *Following is a list of the symbols and abbreviations used:*

dV/Vdt	relative rate of volume increase (h^{-1})
g	specific germination percentage of the seed population (%)
GR	germination rate, or $1/t$ (h^{-1})
GR_g	germination rate of percentage g of the seed population (h^{-1})
GR_{50}	mean germination rate, or $1/t_{50}$ (h^{-1})
L	cell or tissue conductance to water ($MPa^{-1} \cdot h^{-1}$)
m	extensibility coefficient ($MPa^{-1} \cdot h^{-1}$)
ψ_π	osmotic potential (MPa)
$\psi_\pi(g)$	osmotic potential of germination percentage g (MPa)
ψ_p	turgor or pressure potential (MPa)
$\psi_p(g)$	turgor of germination percentage g (MPa)
$\psi_{p,b}$	base, or minimum, turgor permitting germination (MPa)
$\psi_{p,b}(g)$	base, or minimum, turgor permitting germination of percentage g (MPa)
$\overline{\psi}_{p,b}$	mean base turgor, or $\psi_{p,b}(50)$ (MPa)
ψ	water potential of the water source or imbibition medium (MPa)
ψ_i	water potential of the growing cell or tissue (MPa)
ψ_b	base, or minimum, water potential permitting germination (MPa)
$\psi_b(g)$	base, or minimum, water potential permitting germination of percentage g (MPa)
$\overline{\psi}_b$	mean base water potential, or $\psi_b(50)$ (MPa)
$\Delta\psi$	water potential difference, $\psi - \psi_i$ (MPa)
RWC	relative water content, based upon water content after full imbibition on water (%)
σ_{ψ_b}	standard deviation in base water potential within the seed population (MPa)
$\sigma_{\psi_{p,b}}$	standard deviation in base turgor within the seed population (MPa)
t	time to radicle emergence (h)
t_g	time to radicle emergence of germination percentage g (h)
t_{50}	mean time to radicle emergence (h)
$t_g(\psi)$	time to radicle emergence of germination percentage g at a given ψ (h)
θ_H	hydrotime constant, or $(\psi - \psi_b(g))t_g$ (MPa·h)
θ_p	turgor-time constant, or $(\psi_p - \psi_{p,b}(g))t_g$ (MPa·h)
Y	yield threshold, or minimum turgor for growth (MPa)
Y_a	yield threshold, or minimum turgor for growth, of the embryonic axis (MPa)
Y_e	yield threshold, or minimum embryo turgor required for penetration, of the endosperm envelope or other tissues covering the embryonic axis (MPa)

THEORY

The rate of seed germination is the inverse of the time to radicle emergence or the initiation of embryo growth. Since all seeds in a population do not germinate simultaneously, GR must be defined with reference to a particular g. For example, GR_{50} would be the inverse of the time required for radicle emergence of 50% of the seeds in the population ($1/t_{50}$). Linear relationships between GR_g and ψ have been reported (8, 14, 16). Gummerson (14) developed a model to describe seed germination responses to ψ, and included the effects of temperature in the model by using thermal time (*i.e.* a heat-sums or degree-days approach [1]) instead of actual time. However, since I will deal here with a single constant temperature, I will address only the ψ aspects of the model.

Gummerson (14) proposed that a θ_H could be defined as

$$\theta_H = (\psi - \psi_b(g))t_g, \quad (4)$$

where ψ is the seed water potential, $\psi_b(g)$ is the base, or minimum, ψ allowing germination of percentage g, and t_g is the time to germination of percentage g. If θ_H is constant for a seed lot, variation in t_g among germination percentages is in inverse proportion to the difference between ψ and $\psi_b(g)$ of individual seeds. The increasing t_g values of successive fractions of the seed population are therefore a consequence of their increasing $\psi_b(g)$ values. Rearranging Equation 4 gives

$$GR_g = 1/t_g = (\psi - \psi_b(g))/\theta_H, \quad (5)$$

indicating that a plot of $1/t_g$ *versus* ψ should be linear, with an intercept at $1/t_g = 0$ (or complete inhibition of germination at percentage g) equal to $\psi_b(g)$ and a slope of $1/\theta_H$. The slope should be identical for all values of g, since θ_H is a constant, while $\psi_b(g)$ will vary with g. Gummerson (14) determined the distribution of $\psi_b(g)$ by plotting $1/t_g$ *versus* ψ for a range of values of g, finding $\psi_b(g)$ from the intercepts on the ψ axis for each g, then plotting probit (g) as a function of those $\psi_b(g)$ values. The probit transformation linearizes a cumulative normal (Gaussian) distribution, which approximates cumulative germination time courses (7–11, 25). An added feature of a probit plot is that the inverse of the slope of the probit regression line is equal to the standard deviation of the population (11). Thus, θ_H, $\bar{\psi}_b$ (= $\psi_b(50)$, when g = 50% or probit (g) = 0), and σ_{ψ_b} can be estimated. θ_H, $\bar{\psi}_b$, and σ_{ψ_b} are assumed to be constant, intrinsic characteristics of the seed population.

A more convenient method of estimating θ_H, $\bar{\psi}_b$, and σ_{ψ_b} is to adapt a probit procedure described by Ellis *et al.* (10) for determining minimum temperatures for germination. Rearranging Equation 4,

$$\psi_b(g) = \psi - (\theta_H/t_g). \quad (6)$$

Using Equation 6 to estimate the $\psi_b(g)$ of seeds germinating at each t_g, one can plot probit (g) for all observed germination percentages at a range of constant ψs *versus* $\psi - (\theta_H/t_g)$, using different values of θ_H until the best fit, or minimum residual, is obtained in probit analyses. The resulting linear equation will be

$$\text{probit } (g) = [\psi - (\theta_H/t_g) - \bar{\psi}_b]/\sigma_{\psi_b}, \quad (7)$$

which relates g to t_g at any constant ψ. This approach has the advantage that data from all germination percentages at all ψs are utilized in a single regression to identify the optimal value of θ_H. $\bar{\psi}_b$ is determined from the midpoint of the probit line (*i.e.* when probit (g) = 0), and σ_{ψ_b} is the inverse of the slope.

While Equation 7 can be used to predict g as a function of t at any ψ, it would be useful to be able to express germination times at different ψs on a common time scale and reduce the time courses at any ψ to a single curve, just as the transformation to thermal time allows data at all suboptimal temperatures to be expressed as a single curve (1, 7, 9, 10). Since θ_H is a constant, the time to germination varies in direct proportion to $\psi - \psi_b(g)$ (Equation 4). The maximum possible ψ is 0 MPa, so $0 - \psi_b(g)$ represents the maximum range of ψ values allowing germination of percentage g. Normalizing Equation 4 by dividing both sides by $0 - \psi_b(g)$,

$$\theta_H/(0 - \psi_b(g)) = [\psi - \psi_b(g))t_g]/(0 - \psi_b(g)). \quad (8)$$

The left side of this equation is simply $t_g(0)$, the times to germination of seeds in water, while the right side can be reduced to $[1 - (\psi/\psi_b(g))]t_g(\psi)$, where $t_g(\psi)$ is the time to germination of percentage g at any constant ψ. Thus,

$$t_g(0) = [1 - (\psi/\psi_b(g))]t_g(\psi), \quad (9)$$

which states that the times to germination of seeds at any ψ can be normalized to equal the time to germination in water by multiplying $t_g(\psi)$ by the factor $[1 - (\psi/\psi_b(g))]$. When ψ = 0, the factor equals 1, and when $\psi = \psi_b(g)$, the factor reduces to zero and germination does not occur. At any ψ between 0 MPa and $\psi_b(g)$, the relationship between the actual time to germination for any percentage g and the time to germination in water is given by the same factor.

This model provides a quantitative description of the relationship between seed germination rates and ψ. We can compare the parameters derived from this approach to the terms in Equation 1. Germination rate ($GR_g = 1/t_g$) replaces dV/Vdt as the rate term. To convert the driving force ($\psi - \psi_b(g)$) to turgor units, the ψ_p at ψ is equal to $\psi - \psi_\pi$, where ψ_π is the osmotic potential of the embryo at that ψ. The base turgor ($\psi_{p,b}$) is the ψ_p remaining when $\psi = \psi_b$. The variation in GR_g for different fractions of the population embodied in $\psi_b(g)$ could result from variation in $\psi_\pi(g)$ among seeds, or from variation in $\psi_{p,b}(g)$. The extensibility coefficient (m) is formally analogous to $1/\theta_H$, as both act as proportionality constants or slopes relating the rate to the driving force. To convert to turgor units, θ_H is replaced by θ_p, which has the same meaning as θ_H and is estimated by the same procedure, but differs numerically from it as the value of ψ_p differs from that of ψ. Thus, the Lockhart model can be rewritten in terms appropriate to the description of seed germination rates as

$$GR_g = (\psi_p(g) - \psi_{p,b}(g))/\theta_p = (\psi - \psi_\pi(g) - \psi_{p,b}(g))/\theta_p. \quad (10)$$

The relative contributions of variation in $\psi_\pi(g)$ (leading to variation in $\psi_p(g)$) and in $\psi_{p,b}(g)$ to the total variation in GR_g within the population must be experimentally determined. If actual seed germination time courses can be described by this modified Lockhart model, then for a given g, a plot of GR_g as a function of $\psi_p(g)$ should be linear, with a slope of $1/\theta_p$ and an intercept on the turgor axis of $\psi_{p,b}(g)$.

The three terms in Equation 10 that could influence the germination rate are $\psi_p(g)$ $(= \psi - \psi_\pi(g))$, $\psi_{p,b}(g)$, and θ_p, analogous to ψ_p, Y, and m of Equation 1. Factors that alter GR would presumably act by affecting the values of one or more of these parameters. Plots of GR_g *versus* $\psi_p(g)$ would be affected in different ways depending upon variation in each parameter (Fig. 1). If only $\psi_p(g)$ varied among seeds in the population, or was affected by environmental or physiological conditions, the slope and intercept of the plot would be unchanged, and GR_g would vary directly with variation in $\psi_p(g)$ (Fig. 1A). If only $\psi_{p,b}(g)$ was affected, the curve would shift to different intercept values, but with the same slope (Fig. 1B). Variation in the inherent rate of progress toward germination for a given $\psi_p(g)$ and $\psi_{p,b}(g)$ (*i.e.* per unit of 'turgor-time') would appear as a change in slope (Fig. 1C). Equivalent observable effects on GR_g could arise from variation in any of the three parameters. It is also possible that more than one parameter could be influenced by a particular condition. Comparison of GR_g *versus* $\psi_p(g)$ curves of seed lots with and without exposure to conditions that alter GR_g should reveal which of the parameters has been modified.

MATERIALS AND METHODS

Lettuce seeds (*Lactuca sativa* L. cv Empire) were incubated on blotters saturated with PEG 8000 solutions from 0 to −1.2 MPa at 0.2 MPa intervals. The PEG solutions were prepared according to Michel (20), and the ψs were verified using a vapor pressure osmometer (Wescor model 5200) calibrated against NaCl standards. Four replications of 25 seeds each were placed on two 4.5 cm blotters in Petri dishes and moistened with 3.2 mL of water or PEG solution. The dishes were covered with tightly fitting lids to prevent evaporation and were incubated in a germination chamber at 20°C. Incubation was in the dark except for brief intervals when germination was counted under laboratory (fluorescent) light. Counts were made at 2 h intervals during the periods of most rapid germination, and at longer intervals subsequently, until no additional germination was observed for 48 h. Cut seeds were prepared by cutting the seed transversely at approximately one-third the distance from the radicle end to the cotyledon end of the seed. The sections containing the embryonic axes were incubated as described for intact seeds. Germination was scored at emergence and initial gravitropic bending of the radicle for intact seeds, and at the same stage of radicle growth for cut seeds, since the radicle pushed the embryo back from the endosperm cap rather than protruding through it.

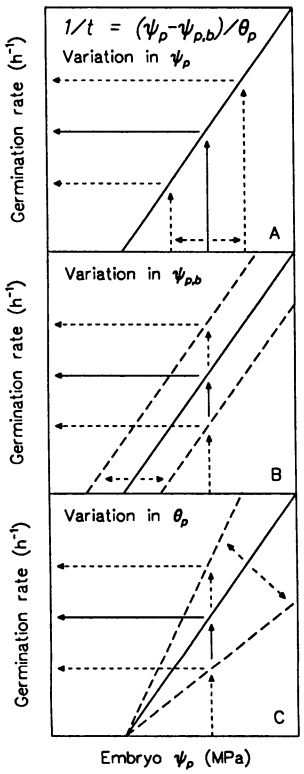

Figure 1. Predicted relationships between seed germination rates (for a given germination percentage) and embryo turgor as influenced by variation in ψ_p (A), $\psi_{p,b}$ (B), or θ_p (C). The *dashed arrows* indicate that equivalent variation in GR around a given value (*solid arrows*) could result from variation in each of the three parameters.

Seed moisture contents at various stages of imbibition were determined by weight loss on oven drying at 130°C for 1 h. The moisture content during the plateau phase of imbibition on water was considered to be 100% RWC and moisture contents at $\psi < 0$ MPa were expressed as percent RWC (3). Embryo osmotic potentials (ψ_π) were determined by thermocouple psychrometry on frozen and thawed tissue using either Merrill-type Peltier-cooled sample chambers or the vapor pressure osmometer. Both types of psychrometers were calibrated with NaCl solutions of known osmotic potential. Seeds were imbibed to the plateau phase of moisture content and were removed from the endosperm envelope by gentle pressure on the cotyledon end. In some cases, the embryos were separated into cotyedons and axes before freezing in sealed microfuge tubes, thawing, and transferring to the psychrometer chambers. All manipulations of embryos were performed in a humidified box to reduce evaporative losses.

Probit analyses were conducted using the PROC PROBIT routine of the SAS statistical package which employs a maximum-likelihood weighted regression method (SAS Institute Inc., Cary, North Carolina) (11). Preliminary analyses were also conducted using standard least-squares linear regression of probit-transformed percentages. It was found that if data greater than 95% of the final germination percentage were excluded (which carry little weight in probit analyses), both methods gave essentially identical estimates of the optimal regression lines.

RESULTS

Germination Responses to ψ

Cumulative germination time courses at a range of ψs were determined for intact (Fig. 2A) and cut (Fig. 2B) lettuce seeds. The data are shown on a logarithmic time scale to separate the time courses at high ψ for clarity, and because the log transformation results in a more normal distribution of ger-

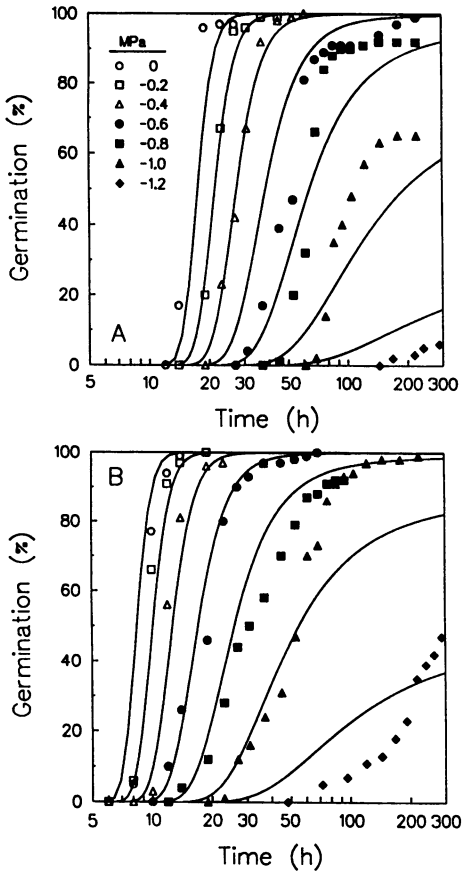

Figure 2. Cumulative germination time courses of intact (A) or cut (B) lettuce seeds incubated at a range of ψs. The time axis is logarithmic in order to separate the curves at high ψ and to normalize the population distributions. The symbols represent the experimental observations, and the solid curves are the cumulative normal distributions predicted on the basis of the hydrotime constants (θ_H) and the means and standard deviations in base ψ (ψ_b and σ_{ψ_b}, respectively) derived from Figure 3 for intact and cut seeds.

mination times (24). Small reductions in ψ delayed germination without reducing the final germination percentage, and further reductions in ψ both delayed and prevented germination of an increasing percentage of the seed population (Fig. 2). Cut seeds, in which the endosperm envelope no longer completely surrounds the embryo, germinated more rapidly at each ψ compared to the intact seeds.

To quantify the water relations parameters of these seeds, the germination percentages were transformed to probits and plotted versus $\psi_b(g) = \psi - (\theta_H/t_g)$, using different values of θ_H in repeated probit analyses until the best fit to all data was obtained (Fig. 3). The optimal values of θ_H (19.3 MPa·h for intact seeds and 9.9 MPa·h for cut seeds) were able to reduce the data at all ψs to single distributions of $\psi_b(g)$. The $\bar{\psi}_b$ and σ_{ψ_b} values for intact and cut seeds were essentially identical (Fig. 3). The ψ_b values estimated from this analysis (-1.10 ± 0.02 MPa for intact and -1.18 ± 0.02 MPa for cut seeds) agreed well with the ψ required to inhibit germination percentage by 50%, interpolated from plots of final germination percentage *versus* ψ (-1.03 and -1.25 MPa for intact and cut seeds, respectively; data not shown). Using the values for θ_H, $\bar{\psi}_b$ and σ_{ψ_b} from Figure 3, the original germination time courses could be predicted by Equation 7, transforming probit (g) back to percentages (Fig. 2). That is, the predicted curves in Figure 2 represent the cumulative normal distributions of the function $[\psi - (\theta_H/t_g) - \bar{\psi}_b]/\sigma_{\psi_b}$ with time at each ψ. The agreement between the predicted and actual values is quite good overall, particularly at the higher ψs. Some discrepancies between predicted and actual percentages occur at the lowest ψs. By systematically varying each of the terms of the function, it was found that increasing θ_H to 25 to 30 MPa·h and allowing ψ to deviate within ± 0.1 MPa from the expected values could account for the differences between the actual and predicted curves at $\psi \leq -0.6$ MPa without altering $\bar{\psi}_b$ or σ_{ψ_b}. An increase in θ_H could be due to slower imbibition at low ψ (3), and the ψ of PEG solutions can easily vary by 0.1 MPa from the predicted values during prolonged incubations. The predicted curves also become very sensitive to small changes in ψ as ψ approaches $\psi_b(g)$, since GR is proportional to $\psi - \psi_b(g)$. A difference in ψ of 0.1 MPa from the expected value changes GR by less than 10% when ψ is near 0 MPa, but the same

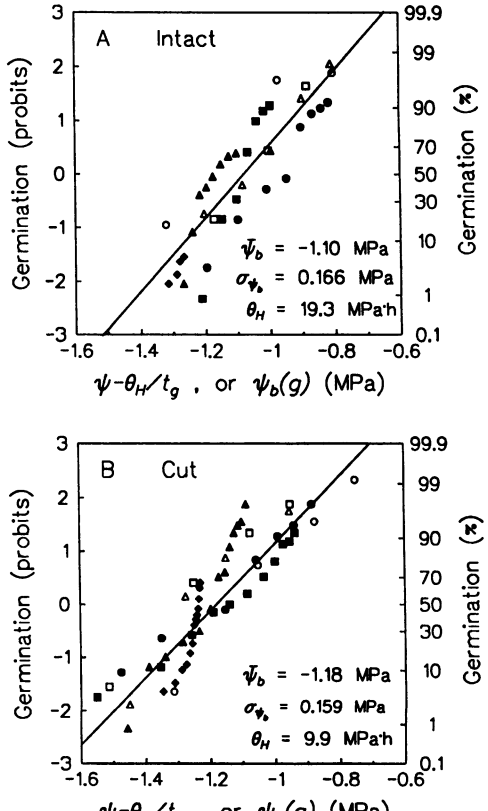

Figure 3. Estimation of the distribution of $\psi_b(g)$ for intact (A) and cut (B) lettuce seeds by probit analyses of cumulative germination data. Cumulative germination percentages at each ψ (symbols as in Fig. 2) were transformed to probits and plotted as functions of $\psi - (\theta_H/t_g)$, which is equivalent to $\psi_b(g)$. Different values of θ_H are used in repeated probit analyses until the best fit (minimum residual) is obtained. The equation for the regression line is probit (g) = $(\psi_b(g) - \bar{\psi}_b)/\sigma_{\psi_b}$, from which $\bar{\psi}_b$ can be calculated (at probit (50) = 0), and σ_{ψ_b} is the inverse of the slope.

variation when $\psi - \psi_b(g) = 0.1$ MPa would either double GR or prevent germination completely. The probit regression technique utilizes data from all germination percentages at all ψs tested to determine the values of θ_H, $\bar{\psi}_b$, and σ_{ψ_b} that best describe the overall population response of germination to ψ.

This point can be further illustrated by plotting the data of Figure 2 on a normalized time scale, or $[1 - \psi/\psi_b(g)]t_g(\psi)$, where $\psi_b(g)$ is the ψ_b predicted for each observed germination percentage, calculated from $\psi - (\theta_H/t_g)$ (see Fig. 3). On this time scale, the germination time courses at all ψs (Fig. 2) are normalized to single curves approximating the time course predicted at 0 MPa (Fig. 4; Eq. 9). Alternatively, the predicted curves of Figure 2 can be generated by dividing the t_g values at $\psi = 0$ MPa by the factor $[1 - \psi/\psi_b(g)]$. This remarkably simple result indicates that both the timing and the final extent of germination are directly proportional to the ratio of ψ to $\psi_b(g)$. The process illustrated in Figure 3 is essentially one of identifying the correct θ_H and distribution of $\psi_b(g)$ that makes this so.

As noted previously, linear relationships have been reported for mean germination rate (GR_{50}) as a function of ψ (8, 14, 16), as would be predicted from Equation 5. When the GR_{50} values from Figure 2 (determined from separate probit analyses of germination percentages at each ψ *versus* log t_g) are plotted versus ψ, the data agree well with the theoretical line, $GR_{50} = (\psi - \bar{\psi}_b)/\theta_H$, using the values of $\bar{\psi}_b$ and θ_H from Figure 3 (Fig. 5A). Parallel curves representing the rates to achieve any g could be similarly constructed using the appropriate value of $\psi_b(g)$ and the same θ_H. Figure 5 illustrates graphically

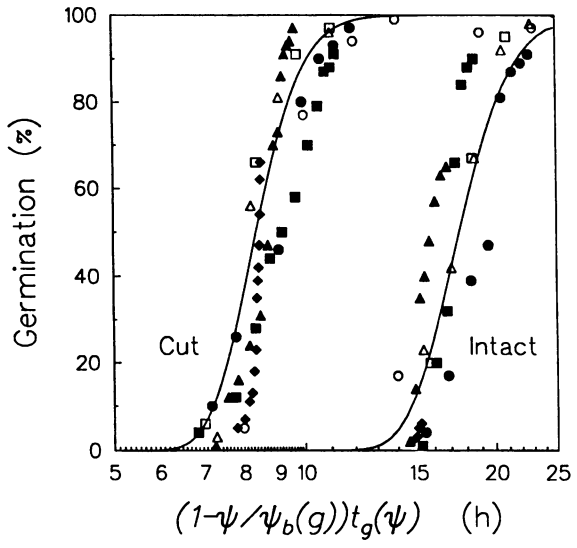

Figure 4. Cumulative germination time courses for intact and cut seeds at a range of ψs (symbols as in Fig. 2) plotted on a normalized time scale. The solid curves represent the predicted time courses in water based upon the parameters derived in Figure 3. When normalized on the basis of $[1 - (\psi/\psi_b(g)]t_g(\psi)$, the families of curves representing germination at different ψs (Fig. 2) collapse to equal the time course in water. Thus, germination at a range of ψs can be expressed on a common normalized scale, as shown here, or the actual time course at any ψ (Fig. 2) can be predicted from that in water according to $t_g(0)/[1 - (\psi/\psi_b(g)]$.

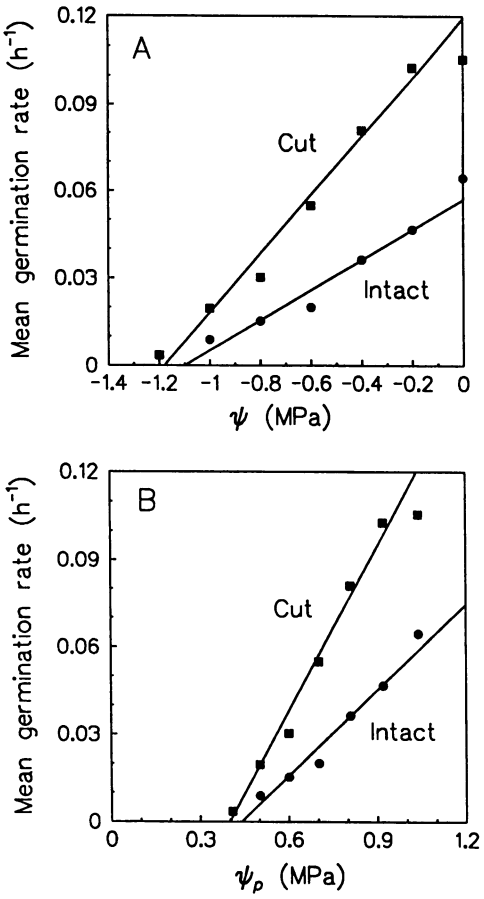

Figure 5. Mean germination rates of intact and cut lettuce seeds as functions of ψ (A) or ψ_p (B). The symbols are the mean germination rates ($1/t_{50}$) at each ψ or ψ_p. The lines are those predicted from the parameters derived as in Figure 3 on the basis of either ψ or ψ_p (*i.e.* $GR_{50} = (\psi - \bar{\psi}_b)/\theta_H$ or $GR_{50} = (\psi_p - \bar{\psi}_{p,b})/\theta_p$). The ψ_p values at each ψ were estimated according to Figure 6.

the conclusion noted earlier, that the difference in germination rates of intact and cut seeds was due primarily to the lower θ_H of the latter, rather than to a significantly lower $\bar{\psi}_b$ for cut seeds.

Germination Responses to ψ_p

To put the model of Figure 5A in terms of ψ_p rather than ψ, $\psi - \psi_\pi(g)$ must be evaluated at each ψ. For the seed lot used here, embryo ψ_π was -1.04 ± 0.03 MPa ($n = 10$), and no significant difference in ψ_π was found between the cotyledons and the embryonic axes. To evaluate whether $\psi_\pi(g)$ varied within the population, embryos were sampled immediately upon radicle protrusion, with successive samples being taken of newly germinated seeds at various times. No significant variation in $\psi_\pi(g)$ was detected among different germination fractions at the time of radicle emergence, and the $\psi_\pi(g)$ values obtained were identical to those from random samples of ungerminated seeds during phase II of imbibition (data not shown). Subsequent calculations therefore assume that single values of ψ_π and ψ_p can be used for all seeds in the

lot during phase II of imbibition. This result also rules out the possibility that variation in $\psi_p(g)$ is responsible for variation in GR_g among seeds in the lot (Fig. 1A).

To estimate ψ_p as a function of ψ, the effect of the change in embryo volume as ψ is reduced must be taken into account. In contrast to most vacuolated plant tissues, relatively small reductions in ψ result in considerable water loss from lettuce seeds (Fig. 6). Assuming that the nonosmotic (apoplastic) volume of the seeds remains constant at 15% over the ψ range under consideration (3), the ψ_π at $\psi < 0$ MPa could be calculated from the change in *RWC* (Fig. 6) by dividing the ψ_π measured in fully imbibed seeds (*RWC* = 100) by the factor [1 − ((100 − *RWC*)/85)]. ψ_p at each ψ was then calculated as $\psi - \psi_\pi$ (Fig. 6, *inset*). Tests where ψ_π was measured directly after equilibration of seeds at low ψ confirmed that correction for changes in osmotic volume estimated the variation in ψ_π with RWC to within 0.1 MPa (Table II).

After calculating the embryo ψ_p at each ψ, the procedure illustrated in Figure 3 was repeated, plotting probit (*g*) *versus* $\psi_p - (\theta_p/t_g)$, optimizing θ_p, and determining $\overline{\psi}_{p,b}$ and $\sigma_{\psi_{p,b}}$. This yielded values for intact seeds of 10.2 MPa·h, 0.44 ± 0.01 MPa, and 0.081 MPa for $\overline{\theta}_p$, $\psi_{p,b}$ and $\sigma_{\psi_{p,b}}$, respectively, and 5.3 MPa·h, 0.40 ± 0.01 MPa and 0.081 MPa for cut seeds. Plotting GR_{50} *versus* ψ_p, the experimental data agreed well with the predicted lines based upon these parameters (Fig. 5B). It is also apparent that the experimental data agree most closely with the theoretical curves where variation in *GR* is due to variation in θ_p (Fig. 1C), rather than to variation in $\psi_{p,b}$ (Fig. 1B).

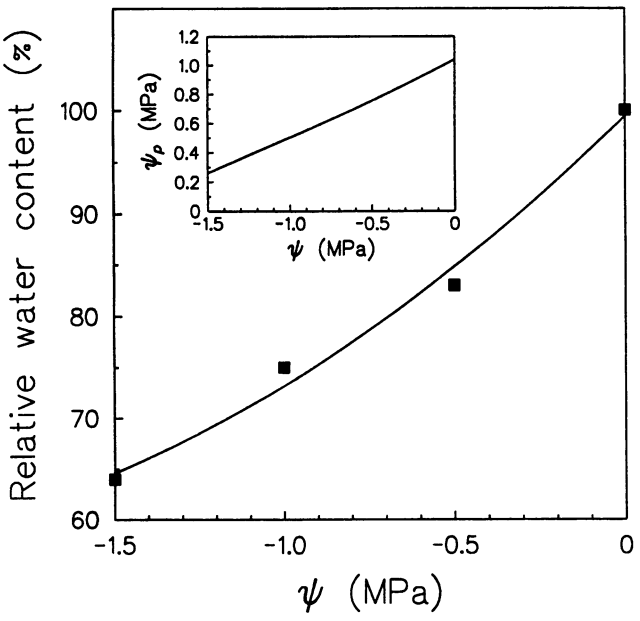

Figure 6. Relationship between seed relative water content and ψ. The moisture contents of seeds imbibed at the indicated ψ are expressed relative to the moisture content of seeds imbibed on water. The regression equation is $RWC = 100 + 32.2\psi + 6\psi^2 (r^2 = 0.99)$. The *inset* shows the relationship between ψ_p and ψ derived on the basis of $\psi_\pi = -1.04$ MPa at full turgor and the reduction in osmotic volume at lower ψ, assuming a constant apoplasic (nonosmotic volume) fraction of 15% *RWC* (3). The equation for the curve is $\psi_p = \psi - (-1.04/(1 - (-32.2\psi - 6\psi^2)/85))$.

Table II. *RWC and Osmotic Potentials (ψ_π)* of Lettuce Seeds Imbibed either on Water or at −1.0 MPa

Seeds were imbibed on water (0 MPa) for 10 h or on −1.0 MPa PEG solution for 68 h before measuring ψ_π by vapor pressure osmometry on frozen and thawed embryos. A subsample of the seeds imbibed on PEG were rinsed and transferred to water (−1.0→0) for an additional 3 h before measurement of water content and ψ_π. Seed water content was determined by the oven method (dry weight basis). The values of ψ_π predicted from the change in *RWC*, assuming a nonosmotic volume of 15%, are shown for comparison with the measured values. Means ± SE are shown ($n = 3$).

Imbibition ψ	Seed Water Content	*RWC*	Measured ψ_π	Predicted ψ_π
MPa	%		*MPa*	
0	76.2 ± 1.5	100	−1.28 ± 0.05	−1.28
−1.0	60.1 ± 3.1	79	−1.76 ± 0.06	−1.70
−1.0→0	72.2 ± 1.0	95	−1.40 ± 0.06	−1.36

DISCUSSION

Since seed germination is evidenced by growth of the embryonic axis, the application of growth models to seed germination should provide information about the factors controlling the rate and extent of germination under various conditions. However, for the reasons discussed in the introduction, the application of cell or tissue growth models to seed germination has been problematic. An individual seed has either germinated (initiated growth) or it has not, *i.e.* germination is a discontinuous or quantal response. The germination responses of a population of seeds can be analyzed in statistical terms, recognizing the variation in the values of specific parameters among seeds that gives rise to different lag times before growth is initiated. This is analogous to the adaptation of cellular water relations models to tissues by defining bulk tissue parameters on a volume-averaged or weight-averaged basis by summing across individual cell types possessing different characteristics (27). As the times to germination of seeds in a population approximate a normal distribution (particularly on a log time scale), statistical approaches based upon the normal distribution, such as the probit transformation, can be applied to analyze the distributions of germination times (7–10, 24). The parameters derived from such analyses (*e.g.* the mean and standard deviation of the population for a particular characteristic) can then be used to estimate the response time of any particular fraction of the population.

The method proposed here extends the model proposed by Gummerson (14) for analyzing seed germination responses to ψ. Gummerson's (14) basic assumption was that the rate of germination is proportional to the difference between ψ and the minimum ψ allowing germination of a particular percentage, $\psi_b(g)$. The variation in times to germination among seeds is a reflection of the differences in their $\psi_b(g)$ values. It is clear that $\psi_b(g)$ does vary within seed populations, as final germination percentages are progressively reduced as ψ is lowered

(Fig. 2) (8, 16, 26, 29, 30). If $\psi_b(g)$ remains constant when the seed population is incubated at different ψs, the time to germination of a particular percentage g at any $\psi > \psi_b(g)$ should be inversely proportional to $\psi - \psi_b(g)$(*cf.* Eq. 5). The proportionality constant, $1/\theta_H$, represents the rate of progress toward germination per unit of hydrotime (MPa·h). The method of repeated probit analyses using different values of θ_H, adapted from that proposed by Ellis *et al.* (10) for determining base temperatures for germination, provides a convenient method of analyzing data from a range of ψs, using the complete germination time courses (Fig. 3). θ_H can also be determined for specific percentage fractions by plotting GR_g *versus* ψ; the slope of the curve is $1/\theta_H$ (Fig. 5A). This approach is useful to get an initial estimate of θ_H, but it does not provide information about the variability of $\psi_b(g)$ unless the analysis is repeated for the entire range of g (14). The probit analysis approach estimates both $\bar{\psi}_b$ and σ_{ψ_b}, which can be used to predict actual germination time courses at any ψ (Fig. 2).

The ability of a single constant value of θ_H to reduce data from a range of ψs to a single distribution of $\psi_b(g)$ (Fig. 3), also evident in the linear relationship between GR_{50} and ψ (Fig. 5A), indicates that $\psi_b(g)$ remained relatively constant during imbibition and incubation at different ψs. This allows normalization of the germination time courses at any ψ to equal that in water using the time scale of $[1 - \psi/\psi_b(g)]t_g(\psi)$ (Fig. 4). In addition, the $\bar{\psi}_b$ values estimated by the current approach were in good agreement with the ψs required to inhibit final germination by 50% in both intact and cut seeds. Thus, similar values were obtained using either probit analyses of time courses or final germination inhibition to estimate $\bar{\psi}_b$. However, this is not always the case; in tomato (*Lycopersicon esculentum* Mill.) seeds, for example, $\bar{\psi}_b$ of cut seeds is dependent upon the ψ at which the seeds are incubated (8). In this case, the germination inhibition approach estimates $\bar{\psi}_b$ values considerably lower than those predicted by probit analysis of germination time courses for seeds imbibed at higher ψs. An advantage of the method presented here is that θ_H, $\bar{\psi}_b$ and σ_{ψ_b} can be estimated from germination time courses at only two or three relatively high ψs where germination still goes to completion and where adaptive changes during incubation are minimized. The parameters obtained from the probit approach at relatively high ψ are more likely to reflect the situation in a seed imbibed in water than are those estimated from germination inhibition experiments conducted at low ψ.

Although θ_H, $\bar{\psi}_b$ and σ_{ψ_b} empirically quantify the germination responses of a seed lot to ψ, it is the physiological basis of these parameters that is of interest. Germination of lettuce seed has been described as being dependent upon a balance of forces between the capacity of the embryonic axis to expand and the ability of the endosperm envelope to resist axis expansion (18, 21, 26, 29). At the end of phase II of imbibition, the driving force for axis expansion is the extent by which ψ_p exceeds Y_a, the yield threshold of the axis cells. The minimum ψ_p allowing axis growth in seeds with the endosperm removed or cut will be an estimate of Y_a. If the endosperm presents a physical constraint to axis expansion, once the axis cells expand sufficiently to become appressed to the endosperm, it will be the yield threshold of the endosperm (Y_e) which limits further expansion, rather than Y_a. During phase II of imbibition, the lettuce endosperm envelope does not limit embryo water uptake, as the water contents of embryos imbibed intact did not increase when removed from the endosperm and transferred to water for short periods prior to the initiation of growth (data not shown). This is in contrast to some other seeds, where the endosperm or testa restrict water uptake by physically limiting the volume of the embryo (8, 15, 30). The minimum ψ_p permitting radicle emergence from intact seeds will be an estimate of $Y_a + Y_e$, or the ψ_p required to expand the radicle cells plus the additional pressure needed to exceed the break strength of the endosperm. For the seed lot used here, the difference in $\bar{\psi}_{p,b}$ values between intact and cut seeds (Y_e) was <0.1 MPa (Fig. 5B), indicating that at the time of radicle emergence, the endosperm did not present a significant mechanical resistance to penetration by the embryo. Thus, endosperm weakening, rather than an increase in ψ_p of the embryo cells as was previously proposed (3, 26), appears to be the factor regulating the timing of radicle emergence. Cytological and morphological changes in the endosperm cells adjacent to the radicle tip occur prior to or coincident with radicle emergence in lettuce and could be related to endosperm weakening (12, 22). The value of Y_e has been shown by the germination inhibition approach to vary among cultivars and seed lots, and with the imbibition temperature and duration (26, 29). For the cultivar and seed lot used here imbibed under optimal conditions, the more rapid germination of cut seeds could be attributed almost entirely to a smaller θ_p, rather than to a reduction in $\bar{\psi}_{p,b}$ (compare Fig. 1, B and C, with Fig. 5B). Of the approximately 9 h reduction in mean time to germination due to cutting (Fig. 4), as much as 3 h could be due to a more rapid initial imbibition rate (shorter phase I) (data not shown). The remaining 6 h reduction in t_{50} may represent the time normally required during phase II for the initiation and completion of the endosperm weakening process. In addition, processes in the axis required for the initiation of growth (such as a reduction in Y_a) might occur more rapidly in cut than in intact seeds due to, *e.g.* greater oxygen availability.

Having shown that seed germination rates can be directly related to the turgor of the embryo (Fig. 5B), it remains to be asked why this should be so. The reason for a relationship between ψ_p and the final extent of germination is clear, since ψ_p must exceed the total yield threshold ($Y_a + Y_e$) in order for germination to occur. When seeds are imbibed at low ψs, however, the rate of germination is slowed even at ψs where final germination is unaffected (Fig. 2). The GR is slowed more than can be accounted for by reduced imbibition rates at low ψ. Lettuce seed imbibition was complete within 24 h even at very low ψ (3), yet germination did not begin until after 60 h at −1 MPa (Fig. 2A). Current evidence indicates that ψ_π is not changing significantly during phase II, even in seeds incubated for extended periods at $\psi < 0$ MPa, if differences in RWC are taken into account (Table I) (8, 15, 23, 29, 30). Since the lettuce axis has to grow only slightly to protrude through the endosperm, it seems unlikely that the delay is

due to a long period of slow growth prior to emergence. The length of phase II would seem to be primarily determined by the time required for $Y_a + Y_e$ to fall below ψ_p. Since cut seeds germinate much more rapidly at any ψ than do intact seeds (Figs. 2 and 4), the time required for a change in Y_e, rather than in Y_a, appears to be the rate-limiting factor in intact seeds. Cracks and breaks between endosperm cells have been observed just prior to visible radicle growth, with the radicle tip apparently forcing the endosperm tissue apart along these cracks (22). This leads to the conclusion that ψ_p of the embryo, or perhaps of the endosperm cells themselves, influences the rate at which processes related to a reduction in Y_e occur. This would be in agreement with the anatomical observations of Georghiou *et al.* (12), who noted that characteristic cellular changes (breakdown of storage materials, vacuole formation) in the endosperm opposite the radicle tip that accompany radicle emergence did not occur if the seeds were incubated for up to 48 h in osmotic solutions that prevented germination.

In conclusion, a method has been presented for analyzing seed germination responses to reduced ψ and for quantifying and predicting seed germination time courses at any ψ on the basis of only three fundamental parameters of the seed lot, θ_H, ψ_b, and σ_{ψ_b}. Germination time courses at a range of ψs can be presented on a normalized time scale based upon the ratio of the test ψ to the $\psi_b(g)$ of seeds in the lot. By estimating embryo ψ_p at various ψs, the same analysis can be used to quantitate the relationship between embryo ψ_p and *GR*. Comparison of intact seeds with seeds where the endosperm envelope has been cut indicates that at the time of radicle emergence, the physical restraint by the endosperm is small. Thus, it does not appear that the embryo forces its way through a considerable barrier, but rather that the endosperm presents only a weak resistance when radicle growth commences. The timing of radicle emergence under optimal conditions is controlled primarily by the rate at which weakening of the endosperm (reduction in Y_e) occurs. The rate of endosperm weakening is apparently sensitive to ψ or ψ_p.

ACKNOWLEDGMENTS

I wish to thank O. Somasco, B.-R. Ni, and A.M. Tarquis for assistance in collecting the experimental data presented in this paper, and K. Shackel and T.C. Hsiao for constructive comments on the manuscript.

LITERATURE CITED

1. **Bierhuizen JF, Wagenvoort WA** (1974) Some aspects of seed germination in vegetables. I. The determination and application of heat sums and minimum temperature for germination. Sci Hortic (Amst) **2:** 213–219
2. **Boyer JS** (1987) Hydraulics, wall extensibility and wall proteins. *In* DJ Cosgrove, DP Knievel, eds, Physiology of Cell Expansion during Plant Growth. American Society of Plant Physiologists, Rockville, MD, pp 109–121
3. **Bradford KJ** (1986) Manipulation of seed water relations via osmotic priming to improve germination under stress conditions. HortScience **21:** 1105–1112
4. **Bradford KJ, Hsiao TC** (1982) Physiological responses to moderate water stress. *In* OL Lange, PS Nobel, CB Osmond, H Ziegler, eds, Encyclopedia of Plant Physiology, New Series, Vol 12B. Springer-Verlag, Berlin, pp 263–324
5. **Carpita NC, Nabors MW, Ross CW, Petretic NL** (1979) Growth physics and water relations of red-light-induced germination in lettuce seeds. III. Changes in the osmotic and pressure potential in the embryonic axes of red- and far-red-treated seeds. Planta **144:** 217–224
6. **Cosgrove DJ** (1986) Biophysical control of plant cell growth. Annu Rev Plant Physiol **37:** 377–405
7. **Dahal P, Bradford KJ, Jones RA** (1990) Effects of priming and endosperm integrity on seed germination rates of tomato genotypes. I. Germination at suboptimal temperature. J Exp Bot **41:** (in press)
8. **Dahal P, Bradford KJ** (1990) Effects of priming and endosperm integrity on seed germination rates of tomato genotypes. II. Germination at reduced water potential. J Exp Bot **41:** (in press)
9. **Ellis RH, Butcher PD** (1988) The effects of priming and 'natural' differences in quality amongst onion seed lots on the response of the rate of germination to temperature and the identification of the characteristics under genotypic control. J Exp Bot **39:** 935–950
10. **Ellis RH, Simon G, Covell S** (1987) The influence of temperature on seed germination rate in grain legumes. III. A comparison of five faba bean genotypes at constant temperatures using a new screening method. J Exp Bot **38:** 1033–1043
11. **Finney, DJ** (1971) Probit Analysis, Ed. 3. Cambridge University Press, Cambridge
12. **Georghiou K, Psaras G, Mitrakos K** (1983) Lettuce endosperm structural changes during germination under different light, temperature, and hydration conditions. Bot Gaz **144:** 207–211
13. **Groot SPC, Karssen CM** (1987) Gibberellins regulate seed germination in tomato by endosperm weakening: a study with gibberellin-deficient mutants. Planta **171:** 525–531
14. **Gummerson RJ** (1986) The effect of constant temperatures and osmotic potential on the germination of sugar beet. J Exp Bot **37:** 729–741
15. **Haigh AM, Barlow EWR** (1987) Water relations of tomato seed germination. Aust J Plant Physiol **14:** 485–492
16. **Hegarty TW** (1976) Effects of fertilizer on the seedling emergence of vegetable crops. J Sci Food Agric **27:** 962–968
17. **Hegarty TW, Ross HA** (1980/81) Investigations of control mechanisms of germination under water stress. Isr J Bot **29:** 83–92
18. **Ikuma H, Thimann KV** (1963) The role of seed-coats in germination of photosensitive lettuce seeds. Plant Cell Physiol **4:** 169–185
19. **Lockhart JA** (1965) Analysis of irreversible plant cell elongation. J Theor Biol **8:** 264–275
20. **Michel BE** (1983) Evaluation of the water potentials of solutions of polyethylene glycol 8000 both in the absence and presence of other solutes. Plant Physiol **72:** 66–70
21. **Nabors MW, Lang A** (1971) The growth physics and water relations of red-light-induced germination in lettuce seeds. I. Embryos germinating in osmoticum. Planta **101:** 1–25
22. **Pavlista AD, Valdovinos JG** (1978) Changes in the surface appearance of the endosperm during lettuce achene germination. Bot Gaz **139:** 171–179
23. **Schopfer P, Plachy C** (1985) Control of seed germination by abscisic acid. III. Effect on embryo growth potential (minimum turgor pressure) and growth coefficient (cell wall extensibility) in *Brassica napus* L. Plant Physiol **77:** 676–686
24. **Scott SJ, Jones RA** (1985) Cold tolerance in tomato. I. Seed germination and early seedling growth of *Lycopersicon esculentum*. Physiol Plant **65:** 487–492
25. **Scott SJ, Jones RA, Williams WW** (1984) Review of data analysis methods for seed germination. Crop Sci **24:** 1172–1174
26. **Takeba G, Matsubara S** (1979) Measurement of growth potential of the embryo in New York lettuce seed under various com-

binations of temperature, red light, and hormones. Plant Cell Physiol **20:** 51–61

27. **Tyree MT, Jarvis PG** (1982) Water in tissues and cells. *In* OL Lange, PS Nobel, CB Osmond, H Ziegler, eds, Encyclopedia of Plant Physiology, New Series, Vol 12B. Springer-Verlag, Berlin, pp 35–77
28. **Watkins JT, Cantliffe DJ** (1983) Mechanical resistance of the seed coat and endosperm during germination of *Capsicum annuum* at low temperature. Plant Physiol **72:** 146–150
29. **Weges R** (1987) Physiological analysis of methods to relieve dormancy of lettuce seeds. PhD dissertation, Agricultural University, Wageningen, The Netherlands
30. **Welbaum GE, Bradford KJ** (1990) Water relations of seed development and germination in muskmelon (*Cucumis melo* L.). V. Water relations of imbibition and germination. Plant Physiol **92:** 1046–1052